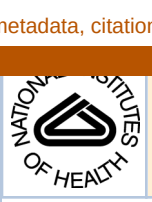

Published in final edited form as:

J Biomech. 2012 January 10; 45(2): 319–325. doi:10.1016/j.jbiomech.2011.10.013.

Mechanical control of spheroid growth: Distinct morphogenetic regimes

Oswaldo A Lozoya[1] and **Sharon R Lubkin**[1,2,*]

[1]Department of Biomedical Engineering, North Carolina State University and University of North Carolina-Chapel Hill, Box 7115, Raleigh, NC 27695-7115

[2]Department of Mathematics, North Carolina State University, Box 8205, Raleigh, NC 27695-8205

Abstract

We develop a model of transport and growth in epithelio-mesenchymal interactions. Analysis of the growth of an avascular solid spheroid inside a passive mesenchyme or gel shows that sustained volumetric growth requires four generic mechanisms: (1) growth factor, (2) protease, (3) control of cellularity, and (4) swelling. The model reveals a bifurcation delineating two distinct morphogenetic regimes: (A) steady growth, (B) growth arrested by capsule formation in the mesenchyme. In both morphogenetic regimes, growth velocity is constant unless and until a complete capsule forms. Comprehensive exploration of the large parameter space reveals that the bifurcation is determined by just two ratios representing the relative strengths of growth and proteolytic activity. Growth velocity is determined only by the ratio governing growth, independent of proteolytic activity. There is a continuum of interior versus surface growth, with fastest growth at the surface. The model provides a theoretical basis for explaining observations of growth arrest despite proteolysis of surrounding tissue, and gives a quantitative framework for the design and interpretation of experiments involving spheroids, and tissues which are locally equivalent to spheroids.

Keywords

mechanics; growth factor; protease; stem cell niche; embryoid body; swelling

INTRODUCTION

The importance of growth regulation cannot be overstated. It exists in simple organisms that can only change size, as well as in complex organisms with complex morphology and differentiated tissues. It is vital in maintaining stem cell niches. It marks the difference between homeostasis and neoplasm. Growth regulation is so fundamental and universal that we would like to understand it from a fundamental level.

*Corresponding author. Office 919-515-1904, fax 919-513-7336, lubkin@eos.ncsu.edu.

The authors have no known conflicts of interest which might inappropriately bias our work.

OAL implemented model, developed model, analyzed data, interpreted model, wrote paper
SRL designed research, developed model, interpreted model, wrote paper

Growth regulation is dependent on both autonomous genetic control and environmental cues, including the mechanics in the microenvironment. In this paper, we focus on the relationship between the chemical and mechanical growth regulatory mechanisms in as simple a system as possible: solid spheroids. Many tissue systems can be modeled as growing solid spheroids, including primitive non-lumened epithelia such as those in branching morphogenesis of salivary gland lobules (Patel et al., 2006) and mammary terminal end buds (Ewald et al., 2008), stem cell niches (Watt and Hogan, 2000), solid avascular carcinomas (Bissell et al., 2002), and embryoid bodies (EB) (Kurosawa, 2007), used in basic research as well as in tissue engineering such as bioprinting (Jakab et al., 2008). In the normal epithelio-mesenchymal relationship, there is continuous regulation of each tissue by the other and by their shared environment. In mesenchyme-free experiments in vitro, an extracellular scaffold is preferred, or the tissue deteriorates. We aim to understand morphogenetic and regulatory phenomena in as general a context as possible, and ask what the commonalities are in native tissues and in simplified systems studied in vitro, i.e. solid confluent spheroids grown in a gel.

In our approach, we are not asking what happens in a specific organism at a specific stage. Rather, we are asking generically what is needed, and what is not, to accomplish a certain task in development. With this *minimalist* or *constructive* approach, we echo the evolutionary path from simple to complex.

This study aims to elucidate the mechanics of generalized epithelio-mesenchymal relationships in morphogenesis, and control of the mechanics by biochemical signals. To this purpose, we developed a mathematical model of the mechanics and control of a growing avascular solid tissue in a passive mesenchyme or gel. The model focuses on regulation of growth by growth factors (GF), availability of raw materials, and availability of compliant space. The mechanisms which regulate growth of a spheroid are some of the lower-level mechanisms that enable higher-level mechanisms to regulate morphogenesis of more complex structures - which may be locally spherical, such as the tip of a cylinder. These growth-regulating mechanisms in a mature organism can make the difference between a stable stem cell niche and a neoplasm. Our purpose in this paper is to ask and perhaps to answer the question, “What are minimal requirements for growing a solid spheroid and halting growth, given the physical world that growing tissues live in?”

There is a large body of mathematical papers exploring generic “tumor growth” simplified to growing spheroids (reviewed in (Araujo and McElwain, 2004; Roose et al., 2007)). Some of the models examine encapsulation (Jackson and Byrne, 2002; Lubkin and Jackson, 2002a; Sherratt, 1999) and growth arrest (Ward and King, 1999a). Many take the same mixture approach as ours (Lubkin and Jackson, 2002a) with a variety of assumptions in the details of the terms for growth regulation and transport (Byrne and Preziosi, 2003; Ward and King, 1997; Ward and King, 1999b). The results depend fairly strongly on some model details such as requiring random migration of cells (Sherratt, 1999) or requiring localized ECM deposition (Jackson and Byrne, 2002), but do not depend on others, such as the use of continuum vs. agent-based (Schaller and Meyer-Hermann, 2006) or hybrid models (Kim et al., 2007). It is important to note that in the vast literature on models of growing spheroids (“tumors”), it is rare to see any parameter estimates or systematic examination of parameter space.

Our model includes ligand and protease activity, and couples them with cellular proliferation and fluid transport. Protease activity is best described as a traditional Michaelis-Menten system (Osenkowski et al., 2004; Remacle et al., 2003; Toth et al., 2002). However, although most existing models also assume Michaelis-Menten kinetics for growth factors, in systems such as EGFR, ligand-dependent growth depends on steady-state levels of receptor

occupancy in cells (Knauer et al., 1984), and is not correctly modeled by Michaelis-Menten kinetics. We have careful estimates for the ranges of all of our parameters, and we perform a systematic exploration of our multidimensional parameter space to estimate model sensitivity.

THE MODEL

Model components

Our model tracks the conservation and transport of generic cells, extracellular matrix (ECM) components, interstitial fluid, growth factors (GF), and proteases. The model further distinguishes between the inner tissue (which, for definiteness, we refer to as epithelium) and the tissue/material surrounding it, either mesenchyme or nonliving culture gel (which, for definiteness, we refer to as mesenchyme). See Figure 1. Model variables and parameters are described in Tables 1 and 2.

Mixture framework

Because we track interstitial fluid flow and tissues of changing density, we use a mixture formulation (Truesdell and Noll, 1965). We model a tissue as containing volume fractions of cells, ECM, and fluid. Because we do not track motion of cells relative to the ECM, we group cells and ECM components into a single phase of volume fraction (cellularity) θ and velocity **v**. The interstitial fluid has volume fraction (porosity) $1-\theta$ and velocity **w**.

Mechanics

Conservation equations for momentum and the model's time-scale assumptions are discussed at length in the Appendix.

Control

The system is controlled by interactions between generic growth factor, protease, and swelling. We track the transport and activity of a generic transmembrane protease, bound to the epithelial cell surface, that digests the mesenchyme. Proteolytic digestion of mesenchyme releases (by solubilization) and activates GF, which is then transported through the aqueous phase. The soluble GF in the aqueous phase is consumed by the epithelium via internalization of ligand-receptor complexes. We neglect endogenous GF synthesis. Further modeling details relating to protease and growth factor are discussed at length in the Appendix.

Crystals grow only at their surface, but soft tissues generally grow *volumetrically* - interior locations move apart from each other. Volumetric growth requires an influx of raw materials, including water. Conservation of mass requires that as a tissue expands, an equal mass of substrates must move into it. This net flow into the tissue is achieved through a variety of mechanisms, including diffusion, vesiculation, pressure-driven flow (swelling) between cells and, at a larger scale, ducts. Physical impediments to transport, e.g. a dense glycocalyx, will inhibit growth. Since inflow of materials is impossible at zero porosity, we assume that a growing tissue has a regulatory mechanism that maintains a small porosity $1-\theta_c$ to allow advection of raw materials (including water) and unbound soluble growth factor G into the tissue. Details are in the Appendix.

We model the local volumetric growth rate as proportional to the persistence level of bound receptors in the epithelium, as in the EGFR system (Dong and Wiley, 2000; Knauer et al., 1984; Wiley et al., 2003).

RESULTS

Requirements for volumetric growth

If epithelium is allowed to grow with zero swelling pressure, its cellular volume fraction increases locally up to saturation, after which growth is confined to the surface. Volumetric growth requires both (a) epithelial target fraction θ_c below 100% and (b) nonzero swelling pressure σ. Without both of these features, new material cannot reach the interior of the epithelium, and growth is restricted to the surface. We refer to the equilibrium cellularity of an epithelium that can still sustain interstitial transport as the *confluence limit*.

Capsule formation and dissolution

As discussed above, when a tissue is growing volumetrically, it is pulling materials into itself. If there is no lumen or vasculature, new material can only come to an epithelium from the interstitium of the surrounding mesenchyme (or gel). As interstitial fluid is drawn into a volumetrically growing epithelium, the neighboring mesenchyme (gel) becomes denser unless it is remodeled at a pace that matches epithelial growth. If the condensing tissue does not remodel itself, and is not dissolved by proteases, it will form a capsule around the growing tissue, as we have previously shown (Lubkin and Jackson, 2002b). This capsule inhibits transport into the epithelium. If the capsule reaches 100% volume fraction, interstitial transport to the epithelium halts, and growth is arrested. Therefore sustained volumetric epithelial growth requires dissolution of the capsule inevitably formed as a byproduct of volumetric growth. The model uses variable protease activity to perform this function.

Distinct morphogenetic regimes

The model exhibits three distinct morphogenetic regimes (Figure 2). In *bulk growth* (BG), the densest tissue is at the center of the spheroid, cellularity remains below the confluence limit everywhere ($\theta e < \theta_c$), and growth is spatially distributed throughout the epithelium. In *surface growth* (SG), the epithelium is of uniform density, at the confluence limit ($\theta e = \theta_c$), and all growth is at the surface. In *capsule formation* (CF), the epithelium is above the confluence limit ($\theta e > \theta_c$), the capsule is densest at the surface, and some of the tissue is pressed centripetally as its interstitial fluid is drawn centrifugally (Supp. Fig. 1). When the capsule reaches 100% cellularity (zero porosity), transport is halted, and growth is arrested.

Bifurcation

In the parameter space tested, surface growth (SG) formed the bifurcation boundary between bulk growth (BG) and capsule formation (CF) (Figure 3). The subset of 8-dimensional parameter space corresponding to SG models was fitted by a compound-exponential function $\Lambda = K_{EG} \exp\left[-(a + b(K_{MR})^c)\right]$ ($a = 1.2$, $b = 0.2$, $c = 0.7$) with $\Lambda = 1$ for SG, $\Lambda < 1$ for BG, and $\Lambda > 1$ for CF. The bifurcation parameter Λ depends on just two nondimensional ratios, for epithelial growth $K_{EG} = \frac{k_I^B S \tau}{T}$ and mesenchyme removal $K_{MR} \equiv \frac{k_{cat}^N C \tau}{F}$. Several of the sampled parameters did *not* influence the bifurcation: tissue modulus of viscosity μ, hydraulic conductivity K_0, ligand diffusivity D_G, latent protease endocytic rate k_H^N, and ligand-receptor dissociation constant K_D^R. Varying the initial cellularities did not qualitatively affect the results.

Surface vs. interior growth

In bulk growth (BG), the ratio Γ_{CS} of mitotic rates at the spheroid core and surface was always less than 1, and went to 0 as the tissue approached the confluence limit (SG) at $\Lambda = 1$

(Figures 3B and 4B). Hence, in BG, much of the growth is at the surface, while in SG, all of the growth is at the surface (Figure 4). Furthermore, the more interstitial space in the epithelium, the higher the fraction of core growth; this is a linear relationship (Figure 3B).

Growth velocity

Although other models simplify their geometry to Cartesian coordinates, our model was in spherical coordinates. However, the epithelial spheroid expanded at a *constant* radial velocity (μm/day) in all cases except when capsule formation had arrested growth (Figure 2). The surface velocity $V_{\theta e}^{S}$ is linear in the nondimensional epithelial growth ratio K_{EG} (Figure 5A): $V_{\theta e}^{S}=pK_{EG}$ (p = 8.1 μm/day, R^2 = 0.93) during steady growth (BG, SG and CF models until capsular growth arrest). The total epithelium content E increases with epithelial surface velocity $V_{\theta e}^{S}$ with a relationship characteristic of a sphere dilating at a constant radial velocity $V_{\theta e}^{S}$, that is, $\Delta E \equiv (E_f - E_0)/E_0 = 3\Psi + 3\Psi^2 + 3\Psi^3$, where $\Psi = V_{\theta e}^{S}(t_f - t_0)/R_0$ (R^2 = 0.998) (Figure 5B).

DISCUSSION

The simple bifurcation criterion provides a guide to the design and interpretation of experiments. For example, if the aim is to grow a spheroid without encapsulation, then ensuring that $\Lambda<1$ ensures that the capsule will not form. That is achieved by reducing K_{EG}, but can also be achieved by increasing K_{MR} (Fig 3C). K_{EG} and K_{MR} can each be regulated independently by regulating several different factors. For example, K_{EG} can be halved experimentally by halving the ligand supply S, doubling the receptor density T, or doubling the bound receptor endocytic rate k_l^B. Some of these manipulations may be substantially easier to perform than others; some are endogenous to the cells and some are external.

We previously showed how swelling pressure creates capsules around a growing epithelium (Lubkin and Jackson, 2002b). In this paper we see how proteases can prevent encapsulation. We show in this paper that the mere presence of proteases is not sufficient; the protease activity K_{MR} must be sufficiently large relative to the epithelial growth K_{EG}. Note that crossing the bifurcation – going from steady growth to capsule formation or vice-versa – may be easier or harder depending on where in parameter space a system begins. For example, the hypothetical system represented by the * in Fig 3C will form a capsule because it has parameters yielding $\Lambda>1$. A 50% reduction in K_{EG} will prevent capsule formation, yet even a 10-fold increase in K_{MR} would not suffice to prevent encapsulation. *The presence of proteases is not sufficient to block encapsulation; the protease activity K_{MR} must be large enough relative to the epithelial growth K_{EG}.* The slope of the bifurcation curve implies that inducing a qualitative change in the system – crossing the bifurcation – is experimentally harder to achieve by changing growth factor or protease kinetics alone. We see this in experiments in which either (a) GF signaling mechanisms or (b) protease activity levels are modified (by gene knock-out, silencing or amplification), but typically not both (a) and (b). Single-variable manipulations mostly modulate the rates of morphogenesis but rarely change the fundamental morphogenetic outcomes.

Specificity and relative importance of model components

The model is constructed from a simplified perspective, with the aim of constructing a minimal mechanism of growth regulation by transport. Tissue mechanical properties do vary over lineage and time, but we focus on a short enough time scale to ignore such changes. The numerous regulatory molecules are lumped into generic “growth factor” and “protease” activities. Real systems are more complex at the cellular level but can for practical purposes be considered in the simplified context of *net* effects. For example, if multiple growth

factors are at work, doubling the *effective* "growth factor activity" may require more than doubling a *specific* growth factor. It is well established that MMPs (matrix metalloproteinases) and their regulators regulate epithelial growth. MMPs are regulated by GF and TIMP (tissue inhibitors of metalloproteinases). Timp-1-reduced mammary epithelia, with greater MMP activity, grew 55% faster than control, and rTimp-1 elevation inhibited growth (Fata et al., 1999). Our simplified (parsimonious) model allows a quantitative interpretation of these experiments and the effect of the experimental factors on the net mesenchyme removal rate K_{MR}.

It is not an essential assumption of our model that the growth factor be bound, released by protease, and subsequently diffuse and advect. A variety of mechanisms can lead to the same morphogenetic gradients (Hammer, 1998). Insoluble growth factors external to the epithelium can be transported into the tissue by being solubilized, vesiculated, probed by filopodia, transported on a motile cell, or induced in a relay (Reilly and Melton, 1996a).

The proteases promote growth in three ways. (1) The GF cannot stimulate the epithelium until the protease releases them from the ECM. Dissolution of the ECM (2) creates more interstitial material, which is then available for conversion to cells, and (3) raises the hydraulic conductivity, enhancing transport of raw materials into the growing tissue.

The epithelial swelling pressure is critical to growth in two ways. First, a tissue cannot grow volumetrically without transport of new material into its interior; this requires the swelling pressure. Second, transport of soluble growth factors into the epithelium is by advection and diffusion. In this context, diffusion is a much slower process than advection, which is why the ligand diffusion coefficient D_G, varied over 4 orders of magnitude in the model, did not affect growth speed or encapsulation. The fluid flow is the product of the hydraulic conductivity and the pressure gradient, regulated by the epithelial swelling pressure.

Systems that are at the bifurcation grow only at their surface, even if their interior has some interstitial space. Because a bifurcation marks a curve in a larger space, a system at a bifurcation will be rare, unless it has been specifically control-engineered to be there. Therefore, spheroids exhibiting steady surface growth and no encapsulation must have some feature not included in our model. For example, we make the point that volumetric growth cannot occur unless there is both interstitial space to permit transport and a swelling pressure to drive it. Systems lacking these features can only grow at the surface, like an evolutionarily primitive stromatolite.

As reviewed in the Introduction, there is a vast literature of models of growing spheroids. What is almost uniformly missing from these models is (a) evidence for the functional form of regulatory terms, (b) parameter values based on experimental evidence, and (c) a parametric study establishing quantitative model dependence on unknown parameter values. In this study we have achieved all three of these.

CONCLUSIONS

The chief finding of this study is the surprisingly simple bifurcation criterion that distinguishes between steady bulk volumetric epithelial growth and capsule-limited growth. Our bifurcation parameter Λ determines whether a spheroid grows indefinitely or halts when capsule completion blocks transport. Although the model was constructed with a large number of parameters (Table 2), the bifurcation parameter Λ delineates regions of a 2-dimensional subset of the 8-dimensional sampled parameter space. Many factors were unimportant in distinguishing bulk growth from capsule formation; for example, tissue

permeability and viscosity. The two key parameters are the nondimensional ratios

$K_{EG} \equiv \frac{k_l^B S \tau}{T}$ and $K_{MR} \equiv \frac{k_{cat}^N C \tau}{F}$ governing epithelial growth and mesenchyme removal.

In tissue engineering, spheroid growth rate is important (Bratt-Leal et al., 2009). The speed of growth in our model was found to be dependent only on K_{EG}, and is linear in K_{EG}. The implications for tissue engineering are clear: to grow tissue rapidly, increase any factor that increases K_{EG}. However, if K_{EG} is above the bifurcation criterion, the growth will be rapid only until encapsulation, when it will halt. Sustainable rapid growth requires not just large K_{EG} but sufficiently large K_{MR} to prevent encapsulation. Thus our study reveals an interesting paradox: a modest increase of growth factor speeds up growth, but too much can *arrest* growth, by outrunning mesenchyme removal.

Supplementary Material

Refer to Web version on PubMed Central for supplementary material.

Acknowledgments

This work was funded by the National Institutes of Health, 1R01GM096195-01 to SRL.

References

Araujo RP, McElwain DLS. A history of the study of solid tumour growth: The contribution of mathematical modelling. Bulletin Of Mathematical Biology. 2004; 66:1039–1091. [PubMed: 15294418]

Barocas VH, Moon AG, Tranquillo RT. The fibroblast-populated collagen microsphere assay of cell traction force--Part 2: Measurement of the cell traction parameter. J Biomech Eng. 1995; 117:161–70. [PubMed: 7666653]

Beysens DA, Forgacs G, Glazier JA. Cell sorting is analogous to phase ordering in fluids. Proc Natl Acad Sci U S A. 2000; 97:9467–71. [PubMed: 10944216]

Bissell MJ, Radisky DC, Rizki A, Weaver VM, Petersen OW. The organizing principle: microenvironmental influences in the normal and malignant breast. Differentiation. 2002; 70:537–546. [PubMed: 12492495]

Boucher Y, Brekken C, Netti PA, Baxter LT, Jain RK. Intratumoral infusion of fluid: estimation of hydraulic conductivity and implications for the delivery of therapeutic agents. Br J Cancer. 1998; 78:1442–8. [PubMed: 9836476]

Bratt-Leal AM, Carpenedo RL, McDevitt TC. Engineering the embryoid body microenvironment to direct embryonic stem cell differentiation. Biotechnology progress. 2009; 25:43–51. [PubMed: 19198003]

Byrne H, Preziosi L. Modelling solid tumour growth using the theory of mixtures. Math Med Biol. 2003; 20:341–66. [PubMed: 14969384]

Chen Y, Schier AF. The zebrafish Nodal signal Squint functions as a morphogen. Nature. 2001; 411:607–10. [PubMed: 11385578]

Chowdhury F, Na S, Li D, Poh YC, Tanaka TS, Wang F, Wang N. Material properties of the cell dictate stress-induced spreading and differentiation in embryonic stem cells. Nat Mater. 9:82–8. [PubMed: 19838182]

David R, Ninomiya H, Winklbauer R, Neumann AW. Tissue surface tension measurement by rigorous axisymmetric drop shape analysis. Colloids Surf B Biointerfaces. 2009; 72:236–40. [PubMed: 19442498]

Dong J, Wiley HS. Trafficking and proteolytic release of epidermal growth factor receptor ligands are modulated by their membrane-anchoring domains. J Biol Chem. 2000; 275:557–64. [PubMed: 10617651]

Ewald AJ, Brenot A, Duong M, Chan BS, Werb Z. Collective epithelial migration and cell rearrangements drive mammary branching morphogenesis. Developmental Cell. 2008; 14:570–581. [PubMed: 18410732]

Fata JE, Leco KJ, Moorehead RA, Martin DC, Khokha R. Timp-1 is important for epithelial proliferation and branching morphogenesis during mouse mammary development. Developmental Biology. 1999; 211:238–254. [PubMed: 10395785]

Flenner E, Marga F, Neagu A, Kosztin I, Forgacs G. Relating biophysical properties across scales. Curr Top Dev Biol. 2008; 81:461–83. [PubMed: 18023738]

Forgacs G, Foty RA, Shafrir Y, Steinberg MS. Viscoelastic properties of living embryonic tissues: a quantitative study. Biophys J. 1998; 74:2227–34. [PubMed: 9591650]

Foty RA, Steinberg MS. The differential adhesion hypothesis: a direct evaluation. Developmental Biology. 2005; 278:255–263. [PubMed: 15649477]

Foty RA, Forgacs G, Pfleger CM, Steinberg MS. Liquid properties of embryonic tissues: Measurement of interfacial tensions. Physical Review Letters. 1994; 72:2298–2301. [PubMed: 10055839]

Foty RA, Pfleger CM, Forgacs G, Steinberg MS. Surface tensions of embryonic tissues predict their mutual envelopment behavior. Development. 1996; 122:1611–20. [PubMed: 8625847]

Francis K, Palsson BO. Effective intercellular communication distances are determined by the relative time constants for cyto/chemokine secretion and diffusion. Proc Natl Acad Sci U S A. 1997; 94:12258–62. [PubMed: 9356436]

Hammer O. Diffusion and Direct Signaling Models are Numerically Equivalent. J Theor Biol. 1998; 192:129–30. [PubMed: 9628845]

Hutson MS, Ma X. Mechanical aspects of developmental biology: perspectives on growth and form in the (post)-genomic age. Preface. Phys Biol. 2008; 5:015001. [PubMed: 18403828]

Jackson TL, Byrne HM. A mechanical model of tumor encapsulation and transcapsular spread. Mathematical Biosciences. 2002; 180:307–328. [PubMed: 12387930]

Jain RK. 1995 Whitaker Lecture: delivery of molecules, particles, and cells to solid tumors. Ann Biomed Eng. 1996; 24:457–73. [PubMed: 8841721]

Jain RK. Transport of Molecules, Particles, and Cells in Solid Tumors. Annual Review Of Biomedical Engineering. 1999; 1:241–263.

Jakab K, Damon B, Marga F, Doaga O, Mironov V, Kosztin I, Markwald R, Forgacs G. Relating cell and tissue mechanics: implications and applications. Dev Dyn. 2008; 237:2438–49. [PubMed: 18729216]

Kalantarian A, Ninomiya H, Saad SM, David R, Winklbauer R, Neumann AW. Axisymmetric drop shape analysis for estimating the surface tension of cell aggregates by centrifugation. Biophys J. 2009; 96:1606–16. [PubMed: 19217876]

Kim Y, Stolarska MA, Othmer HG. A hybrid model for tumor spheroid growth in vitro I: theoretical development and early results. Mathematical Models and Methods in Applied Sciences. 2007; 17(Supp):1773–1798.

Knauer DJ, Wiley HS, Cunningham DD. Relationship between epidermal growth factor receptor occupancy and mitogenic response. Quantitative analysis using a steady state model system. J Biol Chem. 1984; 259:5623–31. [PubMed: 6325444]

Kurosawa H. Methods for inducing embryoid body formation: in vitro differentiation system of embryonic stem cells. Journal of bioscience and bioengineering. 2007; 103:389–398. [PubMed: 17609152]

Lubkin SR, Murray JD. A mechanism for early branching in lung morphogenesis. J Math Biol. 1995; 34:77–94. [PubMed: 8568422]

Lubkin SR, Li Z. Force and deformation on branching rudiments: cleaving between hypotheses. Biomech Model Mechanobiol. 2002; 1:5–16. [PubMed: 14586703]

Lubkin SR, Jackson T. Multiphase mechanics of capsule formation in tumors. Journal of Biomechanical Engineering. 2002a; 124:237–243. [PubMed: 12002134]

Lubkin SR, Jackson T. Multiphase mechanics of capsule formation in tumors. Journal of Biomechanical Engineering. 2002b; 124:237–43. [PubMed: 12002134]

McDowell N, Zorn AM, Crease DJ, Gurdon JB. Activin has direct long-range signalling activity and can form a concentration gradient by diffusion. Curr Biol. 1997; 7:671–81. [PubMed: 9285724]

Mow VC, Kuei SC, Lai WM, Armstrong CG. Biphasic Creep and Stress-Relaxation of Articular-Cartilage in Compression - Theory and Experiments. Journal of Biomechanical Engineering-Transactions of the ASME. 1980; 102:73–84.

Newman SA, Forgacs G, Hinner B, Maier CW, Sackmann E. Phase transformations in a model mesenchymal tissue. Phys Biol. 2004; 1:100–9. [PubMed: 16204827]

Ninomiya H, Winklbauer R. Epithelial coating controls mesenchymal shape change through tissue-positioning effects and reduction of surface-minimizing tension. Nat Cell Biol. 2008; 10:61–9. [PubMed: 18084283]

Norotte C, Marga F, Neagu A, Kosztin I, Forgacs G. Experimental evaluation of apparent tissue surface tension based on the exact solution of the Laplace equation. EPL (Europhysics Letters). 2008:46003.

Osenkowski P, Toth M, Fridman R. Processing, shedding, and endocytosis of membrane type 1-matrix metalloproteinase (MT1-MMP). J Cell Physiol. 2004; 200:2–10. [PubMed: 15137052]

Patel VN, Rebustini IT, Hoffman MP. Salivary gland branching morphogenesis. Differentiation. 2006; 74:349–364. [PubMed: 16916374]

Reilly KM, Melton DA. Short-range signalling by candidate morphogens of the TGF beta family and evidence for a relay mechanism of induction. Cell. 1996a; 86:743–754. [PubMed: 8797821]

Reilly KM, Melton DA. Short-range signaling by candidate morphogens of the TGF beta family and evidence for a relay mechanism of induction. Cell. 1996b; 86:743–54. [PubMed: 8797821]

Remacle A, Murphy G, Roghi C. Membrane type I-matrix metalloproteinase (MT1-MMP) is internalised by two different pathways and is recycled to the cell surface. J Cell Sci. 2003; 116:3905–16. [PubMed: 12915589]

Roose T, Chapman SJ, Maini PK. Mathematical models of avascular tumor growth. Siam Review. 2007; 49:179–208.

Schaller G, Meyer-Hermann M. Continuum versus discrete model: a comparison for multicellular tumour spheroids. Philos Transact A Math Phys Eng Sci. 2006; 364:1443–64. [PubMed: 16766354]

Scholander PF, Hargens AR, Miller SL. Negative pressure in the interstitial fluid of animals. Fluid tensions are spectacular in plants; in animals they are elusively small, but just as vital. Science. 1968; 161:321–8. [PubMed: 5661289]

Sherratt JA. Traveling wave solutions of a mathematical model for tumor encapsulation. Siam Journal On Applied Mathematics. 1999:392–407.

Swabb EA, Wei J, Gullino PM. Diffusion and convection in normal and neoplastic tissues. Cancer Res. 1974; 34:2814–22. [PubMed: 4369924]

Swartz MA, Fleury ME. Interstitial flow and its effects in soft tissues. Annu Rev Biomed Eng. 2007; 9:229–56. [PubMed: 17459001]

Toth M, Hernandez-Barrantes S, Osenkowski P, Bernardo MM, Gervasi DC, Shimura Y, Meroueh O, Kotra LP, Galvez BG, Arroyo AG, Mobashery S, Fridman R. Complex pattern of membrane type 1 matrix metalloproteinase shedding. Regulation by autocatalytic cells surface inactivation of active enzyme. J Biol Chem. 2002; 277:26340–50. [PubMed: 12004057]

Truesdell, C.; Noll, W. The Nonlinear Field Theories of Mechanics. Springer; 1965.

Wan X, Li Z, Lubkin SR. Mechanics of mesenchymal contribution to clefting force in branching morphogenesis. Biomech Model Mechanobiol. 2008; 7:417–26. [PubMed: 17901991]

Ward JP, King JR. Mathematical modelling of avascular-tumour growth. IMA J Math Appl Med Biol. 1997; 14:39–69. [PubMed: 9080687]

Ward JP, King JR. Mathematical modelling of avascular-tumour growth II: modelling growth saturation. Mathematical Medicine and Biology. 1999a; 16:171.

Ward JP, King JR. Mathematical modelling of avascular-tumour growth. II: Modelling growth saturation. IMA J Math Appl Med Biol. 1999b; 16:171–211. [PubMed: 10399312]

Watt FM, Hogan BLM. Out of Eden: stem cells and their niches. Science. 2000; 287:1427. [PubMed: 10688781]

Wiig H, Rubin K, Reed RK. New and active role of the interstitium in control of interstitial fluid pressure: potential therapeutic consequences. Acta Anaesthesiologica Scandinavica. 2003; 47:111–121. [PubMed: 12631039]

Wiley HS, Shvartsman SY, Lauffenburger DA. Computational modeling of the EGF-receptor system: a paradigm for systems biology. Trends Cell Biol. 2003; 13:43–50. [PubMed: 12480339]

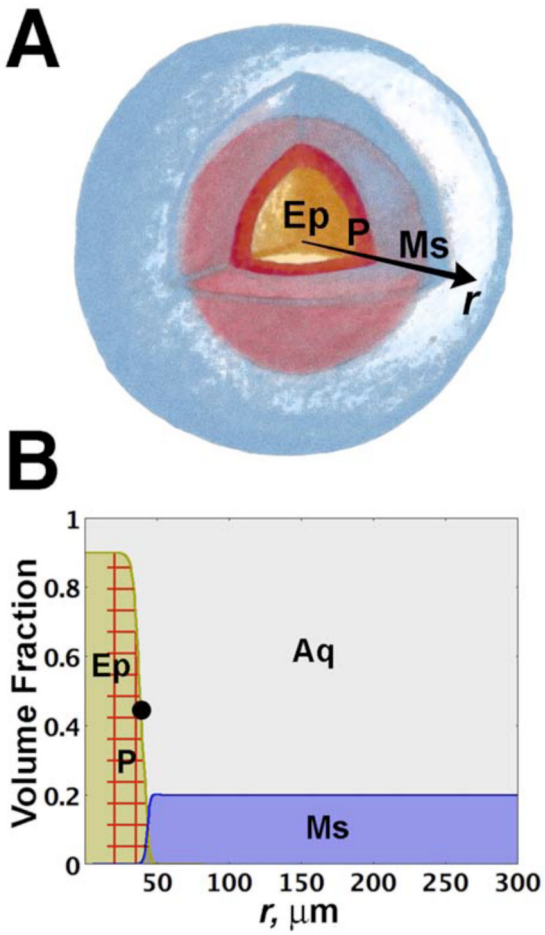

Figure 1.

Geometry and initial conditions in one-dimensional model. (A) Schematic of model domain for epithelium spheroid surrounded by mesenchyme. (B) Radial distributions of initial epithelium (Ep), mesenchyme (Ms) and interstitial aqueous (Aq) phases; grid area highlights region of protease (P) activity. Dot (●) represents location of epithelial surface, $r_{\theta e}^{S}(t)$, defined as where $\theta e = \theta_c/2 = 45\%$.

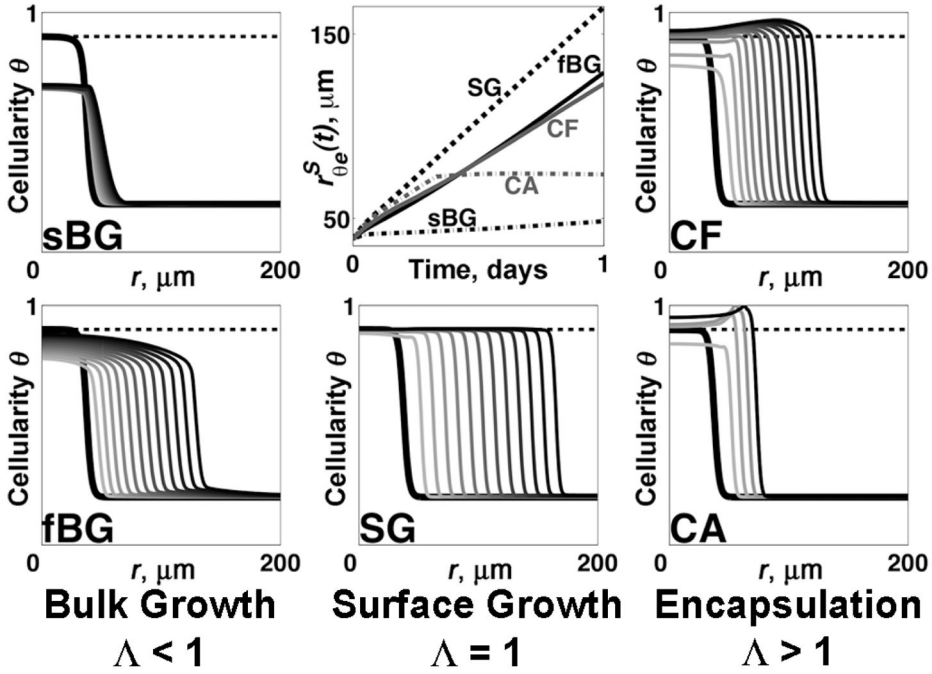

Figure 2.

Time series of cellularity profile showing examples of fundamental morphogenetic outcomes: bulk growth (BG), which can be slow or fast (sBG, fBG); surface growth (SG); capsule formation (CF); and complete capsule with growth arrest (CA). BG is subconfluent ($\theta_{\max} < 90\%$); SG is constant at the confluence limit $\theta_{\max} = \theta_C = 90\%$; CF and CA are superconfluent ($\theta_{\max} > 90\%$). CF progresses to CA as it completes encapsulation ($\theta = 100\%$) at the surface. The surface, defined at $\theta e = \theta_c/2 = 45\%$, exhibits radial displacement that is linear in time ($R^2 = 1$) and corresponds to a constant epithelial surface velocity $V^S_{\theta e}$. The exception is CA models: their overall velocity $V^S_{\theta e}$ is bilinear ($R^2 < 1$) with fast initial displacement followed by immediate stalling after complete encapsulation, thus exhibiting growth arrest. Data in time series plots: solid curve represents initial conditions (same for all models, as described in Figure 1); dashed line is the confluence limit $\theta = \theta_C = 90\%$; curve spacing every 2 hours; all plots correspond to 1 day except for CA displayed until time of arrest.

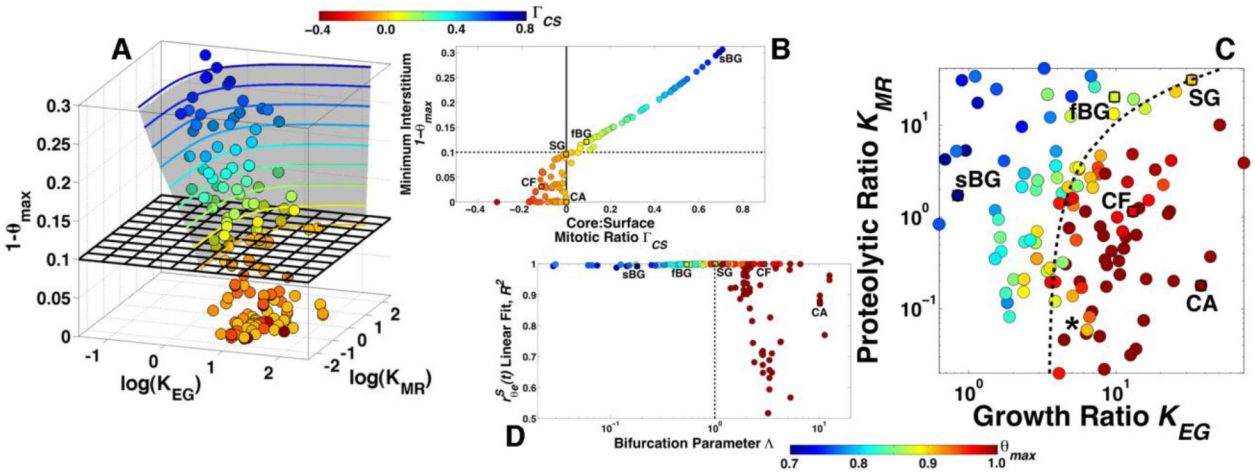

Figure 3.

Morphogenetic bifurcation surface in parameter space. Data correspond to 1 day except for CA models that are displayed in A-C until time of encapsulation. (A) Smooth surface describes the relations among the non-dimensional ratios for epithelium growth and mesenchyme removal K_{EG} and K_{MR}, the core:surface mitotic ratio $\Gamma_{CS} \equiv R^{C}_{EG}/R^{S}_{EG}$ and the minimum observed interstitial fraction $1-\theta_{\max}$. Bifurcation at $\theta_C = 90\%$ (equivalent to $1-\theta_{\max} = 10\%$and corresponding to SG models with $\Gamma_{CS} = 0$) demarcates between subconfluent models with $\Gamma_{CS} > 0$ (BG) and superconfluent models with $\Gamma_{CS} < 0$ (CF and CA). (B) The relationship between $1-\theta_{\max}$ and Γ_{CS} for subconfluent models is linear ($R^2 = 0.98$). (C) The bifurcation in A is fitted by a smooth function $\Lambda = K_{EG}/\exp\left[a+b(K_{MR})^{c}\right]$ in the projected (K_{EG}, K_{MR}) plane ($a = 1.2$, $b = 0.2$, $c = 0.7$) where $\Lambda < 1$ for BG, $\Lambda = 1$ for SG, and $\Lambda > 1$ for CF and CA. Asterisk (*) shows a hypothetical encapsulating system; one could experimentally block its encapsulation by either dramatically increasing K_{MR} or slightly reducing K_{EG}. Square markers correspond to examples from Fig. 2. (D) The bifurcation parameter Λ discriminates between subconfluent models with constant $V^{S}_{\theta e}$ (BG, $\Lambda < 1$, $\theta_{\max} < \theta_C$, $R^2 = 1$ for $r^{S}_{\theta e}(t)$ linear in time) and superconfluent encapsulation models with bilinear spheroid radius $r^{S}_{\theta e}(t)$ (CF and CA, $\Lambda > 1$, $\theta_{\max} > \theta_C$, $R^2 < 1$ for $r^{S}_{\theta e}(t)$ nonlinear in time) as depicted in Figure 2. Colors shown for subconfluent models in A (colormap: Γ_{CS}) and C (colormap: $\theta_{\max}$) are equivalent as a result of the linear correspondence shown in B between Γ_{CS} and $\theta_{\max}$.

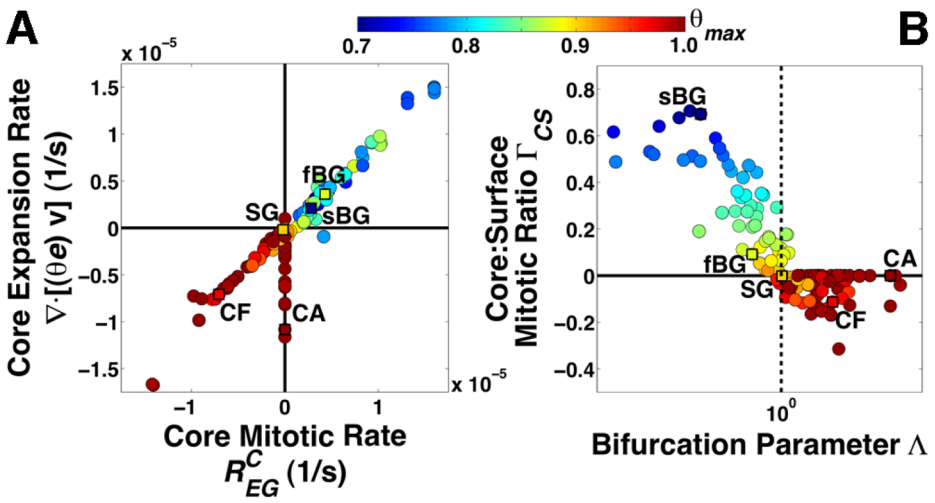

Figure 4.

Growth and expansion of a spheroid distinguish between steady growth and encapsulation mechanics. Square markers correspond to examples from Fig. 2. (A) Measured at the core, epithelium expansion $\nabla\bullet(\theta e\mathbf{v})$ matches the mitotic rate R^C_{EG} during steady bulk growth (BG); surface growth (SG) models show no growth or epithelium flux at the core; capsule formation (CF) both breaks down and compresses core until encapsulation halts transport and growth, when θ reaches 100% (CA). Superconfluent models (CF, CA) have $R^C_{EG} \leq 0$ as a result of the logistic form of growth (carrying capacity defined as the confluence limit θ_C = 90%). (B) The core:surface mitotic ratio $\Gamma_{CS} \equiv R^C_{EG}/R^S_{EG}$ discriminates between BG and SG. The transition between BG and SG corresponds to decreasing growth rate at the spheroid core. All observations from SG models result exclusively from maximal growth at the surface ($\Gamma_{CS} = 0$, $R^S_{EG} > 0$). All data corresponds to 1 day, except for CA models halted at time of encapsulation.

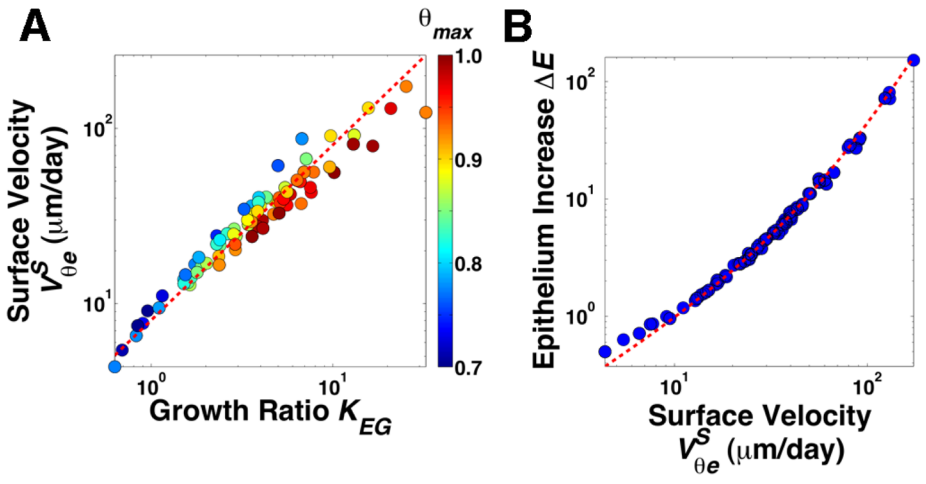

Figure 5.

Surface velocity and volumetric change during steady spheroid growth. (A) The surface velocity is linear in the growth ratio $V^S_{\theta e}=pK_{EG}$ (p = 8.1 μm/day, R^2 = 0.93) during steady growth (BG, SG and CF models). CA models yield piecewise $V^S_{\theta e}$ (Figures 2 and 3D) that halt at complete encapsulation ($\theta_{\max}$ = 100%). (B) The total cellular content of a growing spheroid, represented in terms of the volumetric change ΔE, increases with a relationship characteristic of a sphere dilating at constant surface velocity $V^S_{\theta e}$ (dotted red line, R^2 = 0.99). All data corresponds to 1 day.

Table 1

Model variables

Variable	Symbol	Units
time	t	s
cell velocity	$\boldsymbol{v}$	m/s
interstitial velocity	$\boldsymbol{w}$	m/s
cellularity	θ	-
porosity	$1-\theta$	-
epithelial identity	e	-
mesenchyme or gel identity	$1\text{-}e$	-
epithelial growth rate	R_{EG}	1/s
mesenchyme dissolution rate	R_{MR}	1/s
interphase pressure	P	Pa
hydraulic conductivity	K	Pa
swelling pressure	σ	Pa
effective unbound growth factor activity	G	M
effective substrated protease activity	N	M

Table 2

Parameter values used in multivariate random sampling

Parameter	Symbol	Reported values	Model Values
Sampled			
Tissue shear modulus of viscosity (Beysens et al., 2000; Forgacs et al., 1998; Jakab et al., 2008a; Norotte et al., 2008)	μ	10^4 – 10^7 kg/m-s	10^4 – 10^7 kg/m-s
Hydraulic conductivity (Swartz and Fleury, 2007)	K_0	10^{-14} – 10^{-12} m^3-s/kg	10^{-14} – 10^{-12} m^3-s/kg
Ligand diffusivity (Chen and Schier, 2001; Francis and Palsson, 1997; McDowell et al., 1997; Reilly and Melton, 1996; Wiley et al., 2003)	D_G	0.1 – 100 μm^2/s	0.1 – 100 μm^2/s
Ligand supply from mesenchyme to aqueous phase (Savinell et al., 1989)[1]	S	10–50 pM	100 pM – 1 μM
Transmembrane protease density (Olson et al., 1998)[2]	C	~ 50,000 receptors/cell	4.7 – 470 nM
Protease catalytic rate (Aimes and Quigley, 1995)	k_{cat}^N	16.2 hr^{-1} = 4.5 × 10^{-3} s^{-1}	4.5 × 10^{-4} – 4.5 × 10^{-2} s^{-1}
Latent protease endocytic rate (Jiang et al., 2001; Remacle et al., 2003)	$k_H^N \approx k_I^B$	2.4 × 10^{-3} s^{-1}	2.4 × 10^{-4} – 2.4 × 10^{-2} s^{-1}
Ligand-receptor dissociation constant, steady state EGFR system (Knauer et al., 1984; Starbuck and Lauffenburger, 1992)	K_D^R	4.3 – 4.7 nM	450 pM – 45 nM
Fixed			
Ligand receptors density, steady state EGFR system (Knauer et al., 1984) [3]	T	~ 30,000 receptors/cell	28 nM
Mesenchyme substrate content; collagen in early mesenchymal tissues (Newman et al., 2004)	F	< 5 mg/ml = 20 μM	10 μM
Protease Michaelis constant (Aimes and Quigley, 1995)	K_M^N	8.5 μM	8.5 μM
Bound receptor endocytic rate, steady state EGFR system (Knauer et al., 1984)	k_I^B	2.4 × 10^{-3} s^{-1}	2.4 × 10^{-3} s^{-1}
Specific solvation stress or “swelling pressure” (Jain, 1996; Scholander et al., 1968; Wiig et al., 2003)[4]	h_0	< 10^4 Pa	100 Pa
Epithelial target fraction	θ_C	N/A	90%
Swelling threshold	θ_σ	N/A	65%
Characteristic length	$L = 2R_0$	100 μm	100 μm
Characteristic time (Knauer et al., 1984)[5]	τ	4.7 × 10^4 s = 13 hours	4.7 × 10^4 s

[1] 10–50 pM in media during signaling *in vivo;* Continuous supply at 270 pM *in vitro* induces 100% mitogenic response

[2] Assuming spherical 15-μm diameter cells at ~ 50,000 receptors/cell; 8.3 fmoles per 105 cells; ~ 47 nM

[3] Assuming spherical 15-μm diameter cells at ~ 30,000 receptors/cell; 5.0 fmoles per 105 cells; ~ 28 nM

[4] Up to ~104 Pa (75 mmHg) in neoplastic tissues; much higher than normal tissues

[5] Reference 9-hour doubling rate ≈ 69% of τ under exponential growth